

Micro-strip-line-based sensing chips for characterization of polar liquids in terahertz regime

T. Ohkubo, M. Onuma, J. Kitagawa,^{a)} and Y. Kadoya^{b)}

Department of Quantum Matter, ADSM, Hiroshima University, 1-3-1 Kagamiyama, Higashi-Hiroshima 739-8530, Japan

(Received 7 January 2006; accepted 16 April 2006; published online 26 May 2006)

We have developed embedded thin-film micro-strip-line-based sensor chips working in terahertz regime. In the chip, terahertz waves are generated and detected with femtosecond optical pulses accessed from the back side of the chips. Moreover, the spectroscopic sensitivity can be freely adjusted by changing the thickness of a polyimide cover layer. They make it easy to measure polar liquids. The measurement of water is demonstrated with spectral range from 30 GHz to 1–1.5 THz, where the upper limit depends on the thickness of the cover layer. © 2006 American Institute of Physics. [DOI: 10.1063/1.2207989]

Recent remarkable progress in the technologies for emitting and detecting terahertz waves has enabled us to characterize various materials in terahertz range. As a sensing technique with terahertz waves, the transmission free-space terahertz spectroscopy has widely spread. However, it is in general difficult to characterize polar liquids because of their strong absorption, while the reflection geometry needs a rather complicated specimen cell.¹ To overcome the difficulty, the attenuated-total-reflection method has been developed recently.²

Waveguide-based sensor chips which are used in gigahertz range^{3,4} are also promising way to detect polar liquids. To realize the sensing method in terahertz range, solid state transmission lines are desired, which justly conduct downsizing and functionalization⁵ being obviously important issues in terahertz technologies. A few pioneer works of such a technique have been reported.^{6,7} In particular, Nagel *et al.* have proposed a thin-film micro-strip-line (MSL)-based sensing technique with a resonator which would be excellent to detect a DNA hybridization at femtomolar levels.⁷

In this letter, we propose embedded MSLs where MSLs are covered with a polymer thin film, possessing a further significant merit: the controllability of the interaction between specimens and the terahertz waves. It is particularly effective for the measurement of polar liquids as will be demonstrated. In addition, our device is designed so as to allow optical access from the back side of chips. Such a chip would open a new door to more general-purpose sensing with terahertz waves applicable to various polar materials. We demonstrate the terahertz spectroscopic performance of developed embedded thin-film MSL-based sensor chips by measuring the water.

The basic structure of the embedded MSL is schematically depicted in Figs. 1(a) and 1(b). As the ground plane, a 0.2- μm -thick Au film was deposited on a glass substrate. In the film, small holes were opened to allow the optical access from the back side of the chip. The commercial polyimide (PI) precursor (TORAY Semicofine, SP-483) was spin coated and thermally cured to form a transmission layer with 20 μm thickness. Then, small pieces of low-temperature-grown

GaAs thin films, which are used as the photoconductive (PC) switches, were placed on the PI layer by the van der Waals bonding technique. The distance between the PC switches is 1 mm. A 20- μm -wide signal line made of Au was formed using conventional photolithography and lift-off method. Finally, as a cover layer, PI is again coated. We have prepared four kinds of chips where the thicknesses, d 's, of the PI cover layers are 3, 7, 10, and 12 μm , respectively. The d 's are determined by measuring the thicknesses of PI films formed on GaAs substrates with the same condition as those for the present chips after the cleavage of the GaAs substrates. But we notice that a deviation from the true thickness might occur. For the measurement of water, a polyethylene vessel with an inner diameter of 6 mm (capacity of 0.14 cm^3) was

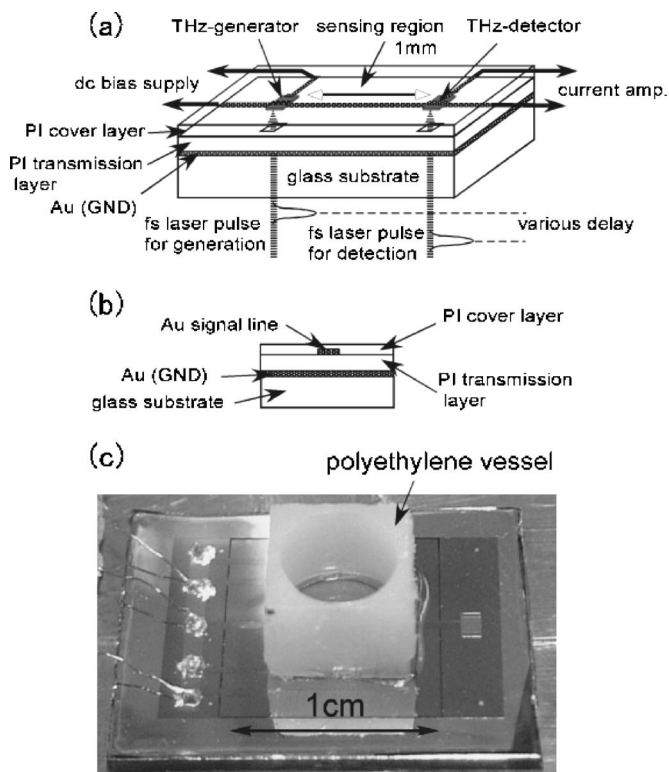


FIG. 1. (a) Schematic view of the MSL structure in the developed chip. Polyethylene vessel is not drawn. (b) Cross section of the MSL. (c) Photograph of the sensor chip.

^{a)}Electronic mail: jkita@hiroshima-u.ac.jp

^{b)}Electronic mail: kd@hiroshima-u.ac.jp

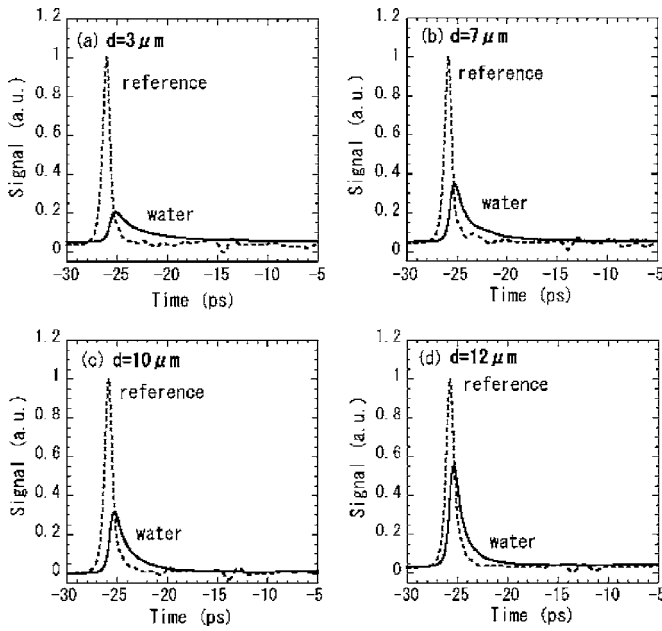


FIG. 2. Time evolution of terahertz pulses with and without water.

glued on the chip in a way that it involves the whole sensing region including the PC gaps as shown in the photograph [Fig. 1(c)].

Terahertz pulses were generated at a PC switch biased with 40 V and excited from the back side of the chip by optical pulses from a mode-locked Ti-sapphire laser with a central wavelength of 810 nm and duration of 200 fs at a pulse repetition rate of 76 MHz. Terahertz pulses propagating along the transmission line were then detected by another PC switch triggered by time-delayed pulses of the laser.

In Fig. 2, terahertz wave forms with and without water (denoted as reference) are shown. The peak intensities of all reference signals are normalized to 1. In each reference signal, parasitic peaks are observed about 12 ps after the arrival of the main pulses. By using roughly estimated effective refractive index $n_{\text{eff,ref}}(1.6-1.7)$ of an unloaded transmission line as mentioned below, the retardation corresponds to a 2 mm length propagation. Therefore this anomaly can be ascribed to an extra terahertz pulse reflection between the PC switches. Terahertz wave signal is attenuated heavily by the water and becomes broader compared to reference one. The wave form of the chip with $d=7 \mu\text{m}$ for the water is almost identical to that with $d=10 \mu\text{m}$. This indeed indicates that the thicknesses of the PI cover layer for both chips are closer than the designed value albeit our careful fabrications, and that a more sophisticated technique for the stable thickness control is needed. Considering that the terahertz pulses in Figs. 2(b) and 2(c) are representing that of a chip with d ranging from 7 to $10 \mu\text{m}$, the peak intensity is successively reduced with decreasing d . It is accompanied by the more delayed time from the reference signal and the more broadened wave form. These facts strongly suggest that the interaction between the water and the terahertz waves can be certainly controlled by slightly changing the d : the thinner the PI cover layer is, the stronger the water induced absorption of terahertz waves is.

The frequency dependencies of the variation of n_{eff} due to the water $\Delta n_{\text{eff,w}}$ and the amplitude absorption coefficient $\alpha_{\text{eff,w}}$ of the water are determined as

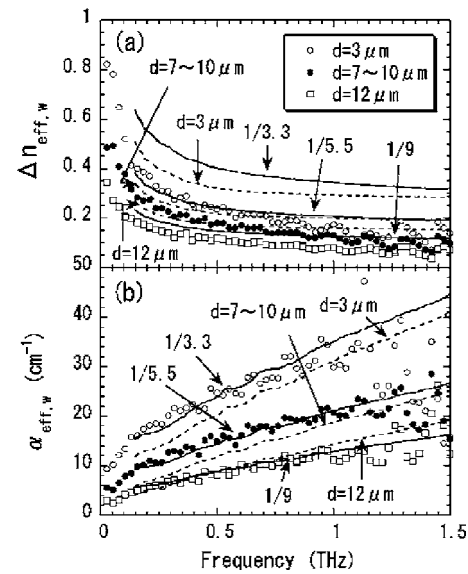


FIG. 3. (a) $\Delta n_{\text{eff,w}(f)}$ and (b) $\alpha_{\text{eff,w}(f)}$ for chips with $d=3, 7 \sim 10$, and $12 \mu\text{m}$. Symbols are the experimental results. Solid and broken curves are numerical estimations using two simple methods.

$$\Delta n_{\text{eff,w}(f)} = \frac{c \Delta \phi(f)}{2 \pi f L}, \quad (1)$$

$$\alpha_{\text{eff,w}(f)} = -\frac{1}{L} \ln \left| \frac{E_w(f)}{E_{\text{ref}}(f)} \right|, \quad (2)$$

where $E_w(f)$ [$E_{\text{ref}}(f)$] means the complex terahertz electric field in the frequency domain with water (reference), $\Delta \phi$ the phase shift of E_w from E_{ref} , L is the sensing length of 1 mm, and c the speed of light. The symbols shown in Fig. 3 are thus obtained $\Delta n_{\text{eff,w}(f)}$'s and $\alpha_{\text{eff,w}(f)}$'s. The spectral range is from 30 GHz up to about 1.5 THz where the upper frequency is limited down to 1 THz in the chip with $d=3 \mu\text{m}$ as demonstrated by the downward deviation of $\alpha_{\text{eff,w}}$ above 1 THz. The deviation can be ascribed to the Fourier transformed spectra for $f > 1$ THz being near to the noise floor (not shown). The $\Delta n_{\text{eff,w}(f)}$ and $\alpha_{\text{eff,w}(f)}$ for $d=7-10 \mu\text{m}$ are represented by those with $d=10 \mu\text{m}$, as the almost identical terahertz signals of water between the chip with $d=7 \mu\text{m}$ and that with $d=10 \mu\text{m}$ lead to the same $\Delta n_{\text{eff,w}(f)}$ and $\alpha_{\text{eff,w}(f)}$. The small upturn occurs in $\Delta n_{\text{eff,w}(f)}$ with decreasing frequency, which is conspicuous with decreasing d and reflects the dispersion of the refractive index of the water. Going from the chip with $d=12 \mu\text{m}$ to that with $d=3 \mu\text{m}$, $\alpha_{\text{eff,w}(f)}$ evolves over the measured frequency range. The $\Delta n_{\text{eff,w}(f)}$'s and $\alpha_{\text{eff,w}(f)}$'s being smaller than the reported values ($\sim 1.15 = n_{\text{water}} - n_{\text{air}}$ and $\sim 110 \text{ cm}^{-1}$ at 1 THz, for example)^{1,2} for the water, result from the reduced interaction with terahertz waves in the present chip. Furthermore, d dependencies of $\Delta n_{\text{eff,w}}$ and $\alpha_{\text{eff,w}}$ significantly imply the controlled interaction between the water and the terahertz waves.

Although no fully satisfied analytical expressions for terahertz transmission properties of MSLs exist, the $\Delta n_{\text{eff,w}(f)}$'s and $\alpha_{\text{eff,w}(f)}$'s have been evaluated by two simple methods: the adjusting of values determined by terahertz spectroscopy¹ with a constant multiplication factor, A , and the utilization of formulas applicable to gigahertz range. The values calculated by the first method are represented by solid curves in Fig. 3 for $A=1/3.3, 1/5.5$, and $1/9$ that are chosen

to reproduce the $\alpha_{\text{eff},w}(f)$'s well. The A 's are consistent with those obtained from a result by a finite-difference time-domain calculation. For $\Delta n_{\text{eff},w}$, the refractive index of the air is subtracted before the multiplication. According to the second method, for a multilayer MSL containing a transmission layer (complex dielectric permittivity: ϵ_{di}^* , thickness: $h = 20 \mu\text{m}$), cover one (ϵ_{di}^* , d) and specimen one (ϵ_s^* , ∞), $\Delta n_{\text{eff},w}(f)$ and $\alpha_{\text{eff},w}(f)$ caused by the dielectric loss can be calculated as follows:^{8,9}

$$\Delta n_{\text{eff},w}(f) = \sqrt{\epsilon_{\text{eff}}^*(f) - n_{\text{eff,ref}}(f)}, \quad (3)$$

$$= \text{Re} \left[\sqrt{\epsilon_{\text{di,eq}}^* - \frac{\epsilon_{\text{di,eq}}^* - \epsilon_{\text{eff}}^*}{1 + P(f)}} \right] - n_{\text{eff,ref}}(f), \quad (4)$$

$$\alpha_{\text{eff},w}(f) = \frac{13.7}{\lambda} \frac{\epsilon_{\text{di,eq}} \left[\epsilon_{\text{eff}}(f) - 1 \right] \text{Im}(\epsilon_{\text{di,eq}}^*)}{\sqrt{\epsilon_{\text{eff}}(f) (\epsilon_{\text{di,eq}} - 1)} \epsilon_{\text{di,eq}}}, \quad (5)$$

$$\epsilon_{\text{di,eq}}^* = \frac{\epsilon_{\text{eff}}^* - 1}{q} + 1, \quad (6)$$

$$\epsilon_{\text{eff}}^* = \frac{C^*}{C_0}, \quad (7)$$

$$\frac{1}{C^*} = \frac{1}{\pi \epsilon_0} \int_0^\infty \frac{F(\beta)^2}{\beta Y^*} d\beta, \quad (8)$$

$$Y^* = \epsilon_{\text{di}}^* \coth(\beta h) + \epsilon_{\text{di}}^* \frac{\epsilon_s^* + \epsilon_{\text{di}}^* \tanh(\beta d)}{\epsilon_{\text{di}}^* + \epsilon_s^* \tanh(\beta d)}, \quad (9)$$

where $n_{\text{eff,ref}}(f)$ is $\sqrt{\epsilon_{\text{eff}}^*(f)}$ with $\epsilon_s^* = 1$, $P(f)$ represents the structural dispersion,¹⁰ $\epsilon_{\text{di,eq}}$ and ϵ_{eff} are the real part of $\epsilon_{\text{di,eq}}^*$ and ϵ_{eff}^* , respectively, λ is the wavelength in free space, q is the filling factor,⁸ ϵ_0 is the vacuum permittivity, C_0 is calculated by substituting $\epsilon_{\text{di}}^* = \epsilon_s^* = 1$ to Eq. (8), and $F(\beta)$ is given by Yamashita.¹¹ These equations are derived by reducing multilayer structures to an equivalent single layer MSL combined with the structural dispersion and applicable up to 100 GHz.^{8,9} The unit of $\alpha_{\text{eff},w}(f)$ is dB/unit length. The ϵ_{di}^* of PI was tentatively fixed as a dispersionless and absorptionless (measured $\tan \delta$ is only about 0.03) constant value of 2.89 which is preliminary determined by our free-space terahertz spectroscopic system. The broken curves in Fig. 3 are

thus calculated $\Delta n_{\text{eff},w}$'s and $\alpha_{\text{eff},w}$'s for each chip. In the case of the chip with $d \sim 7 \sim 10 \mu\text{m}$, the averaged value of $8.5 \mu\text{m}$ is used. As shown in Fig. 3, both methods semiquantitatively explain the experimental $\Delta n_{\text{eff},w}$'s and $\alpha_{\text{eff},w}$'s. Especially $\alpha_{\text{eff},w}(f)$ can be reproduced rather well including the frequency dependence, while the deviations in $\Delta n_{\text{eff},w}(f)$'s remain large even if other A 's have forced a smaller residual in the first method. Although the origin of the deviations in Δn_{eff} 's is not clear at present, we note that $\alpha_{\text{eff}}(f)$ would give sufficient guidelines in the characterization of polar materials.

In conclusion, we have developed embedded thin-film MSL-based sensor chips working in terahertz regime and the demonstration was performed by measuring the water. The sensitivity can be easily controlled by adjusting the thickness of the PI cover layer. In our developed sensors, the optical access from the back side of chips is achieved. Since in principle the light pulses can be delivered with optical fibers for emitting and detecting terahertz waves, these kinds of chips may be a good candidate for remote sensor heads of the terahertz spectroscopy systems.

This work was supported by Strategic Information and Communications R&D Promotion Programme of Ministry of Public Management, Home Affairs, Posts and Telecommunications, Japan.

¹C. Rønne, L. Thrane, P.-O. Åstrand, A. Wallqvist, K. V. Mikkelsen, and S. R. Keiding, *J. Chem. Phys.* **107**, 5319 (1997).

²H. Hirori, K. Yamashita, M. Nagai, and K. Tanaka, *Jpn. J. Appl. Phys., Part 2* **43**, L1287 (2004).

³W. B. Weir, *Proc. IEEE* **62**, 33 (1974).

⁴A. M. Nicolson and G. F. Ross, *IEEE Trans. Instrum. Meas.* **IM-19**, 377 (1970).

⁵K. Takase, T. Ohkubo, F. Sawada, D. Nagayama, J. Kitagawa, and Y. Kadoya, *Jpn. J. Appl. Phys., Part 2* **44**, L1011 (2005).

⁶R. Sprik, I. N. Duling III, C.-C. Chi, and D. Grischkowsky, *Appl. Phys. Lett.* **51**, 548 (1987).

⁷M. Nagel, P. H. Bolivar, M. Brucherseifer, H. Kurz, A. Bossert, and R. Büttner, *Appl. Phys. Lett.* **80**, 154 (2002).

⁸A. K. Verma and G. H. Sadr, *IEEE Trans. Microwave Theory Tech.* **40**, 1587 (1992).

⁹A. K. Verma and A. Bhupal, *Microwave Opt. Technol. Lett.* **17**, 368 (1998).

¹⁰M. Kirschning and R. H. Jansen, *Electron. Lett.* **18**, 272 (1982).

¹¹E. Yamashita, *IEEE Trans. Microwave Theory Tech.* **MTT-16**, 529 (1968).